

Excitation energies along a range-separated adiabatic connection

Elisa Rebolini^{1,2,*}, Julien Toulouse^{1,2,†}, Andrew M. Teale^{3,4}, Trygve Helgaker⁴, and Andreas Savin^{1,2,‡}

¹*Sorbonne Universités, UPMC Univ Paris 06, UMR 7616,
Laboratoire de Chimie Théorique, F-75005 Paris, France*

²*CNRS, UMR 7616, Laboratoire de Chimie Théorique, F-75005 Paris, France*

³*School of Chemistry, University of Nottingham,
University Park, Nottingham NG7 2RD, United Kingdom*

⁴*Centre for Theoretical and Computational Chemistry,
Department of Chemistry, University of Oslo,
P.O. Box 1033 Blindern, N-0315 Oslo, Norway*

(Dated: July 9, 2014)

We present a study of the variation of total energies and excitation energies along a range-separated adiabatic connection. This connection links the non-interacting Kohn–Sham electronic system to the physical interacting system by progressively switching on the electron–electron interactions whilst simultaneously adjusting a one-electron effective potential so as to keep the ground-state density constant. The interactions are introduced in a range-dependent manner, first introducing predominantly long-range, and then all-range, interactions as the physical system is approached, as opposed to the conventional adiabatic connection where the interactions are introduced by globally scaling the standard Coulomb interaction. Reference data are reported for the He and Be atoms and the H₂ molecule, obtained by calculating the short-range effective potential at the full configuration-interaction level using Lieb’s Legendre-transform approach. As the strength of the electron–electron interactions increases, the excitation energies, calculated for the partially interacting systems along the adiabatic connection, offer increasingly accurate approximations to the exact excitation energies. Importantly, the excitation energies calculated at an intermediate point of the adiabatic connection are much better approximations to the exact excitation energies than are the corresponding Kohn–Sham excitation energies. This is particularly evident in situations involving strong static correlation effects and states with multiple excitation character, such as the dissociating H₂ molecule. These results highlight the utility of long-range interacting reference systems as a starting point for the calculation of excitation energies and are of interest for developing and analyzing practical approximate range-separated density-functional methodologies.

I. INTRODUCTION

Range-separated density-functional theory (see, e.g., Ref. 1) constitutes an interesting alternative to standard Kohn–Sham (KS) density-functional theory (DFT) [2, 3]. In the standard KS approach, the physical interacting electronic Hamiltonian is replaced by an effective non-interacting Hamiltonian. By contrast, in range-separated DFT, the physical Hamiltonian is instead replaced by a partially interacting Hamiltonian that incorporates the long-range part of the electron–electron interaction. This corresponds to an intermediate point along a range-separated adiabatic connection [1, 4–7]. The KS Hamiltonian is linked to the physical Hamiltonian by progressively switching on the long-range part of the two-electron interaction, whilst simultaneously modifying the one-electron potential so as to maintain a constant ground-state density. The ground-state energy of the physical system can then be extracted from the

ground state of the long-range interacting Hamiltonian by using a short-range density functional describing the complementary short-range part of the electron–electron interaction. Be aware that this range-separated manner of introducing the interaction is not the usual way of performing the adiabatic connection, where the Coulomb interaction is instead scaled by a multiplicative constant going from 0 to 1.

Several short-range density-functional approximations have been developed [1, 4, 8–13] and a diverse range of approaches for calculating the ground state of the long-range interacting Hamiltonian have been explored. To aid in the description of static (or strong) correlation effects, which are poorly treated by standard density functionals, configuration-interaction [1, 4, 7, 14–17], multiconfiguration self-consistent-field (MCSCF) [18–20], density-matrix functional theory (DMFT) [21–23], and constrained-pairing mean-field theory [24, 25] descriptions of the long-range interacting systems have been employed. To treat van der Waals interactions, second-order perturbation theory [26–37], coupled-cluster theory [11, 13, 38–40], and random-phase approximations [41–51] have been used successfully.

Electronic excitation energies can also be calcu-

*Electronic address: rebolini@lct.jussieu.fr

†Electronic address: julien.toulouse@upmc.fr

‡Electronic address: savin@lct.jussieu.fr

lated in range-separated DFT by using the linear-response approach with a time-dependent generalization of the static ground-state theory [52]. In this case, the excitation energies of the long-range interacting Hamiltonian act as starting approximations that are then corrected using a short-range density-functional kernel, just as the KS excitation energies act as starting approximations in linear-response time-dependent density-functional theory (TDDFT). Several such range-separated linear-response schemes have been developed, in which the short-range part is described by an approximate adiabatic semi-local density-functional kernel and the long-range linear-response part is treated at the Hartree–Fock [52–55], MCSCF [52, 55], second-order polarization-propagator approximation (SOPPA) [55], or DMFT [56] levels. These schemes aim at overcoming the limitations of standard linear-response TDDFT applied with usual adiabatic semi-local approximations for describing systems with static correlation [57], double or multiple excitations [58], and Rydberg or charge-transfer excitations [59, 60].

For the purpose of analyzing linear-response range-separated DFT approaches, it is desirable to have accurate reference values of the excitation energies of the long-range interacting Hamiltonian along the range-separated adiabatic connection [cf. Eq. (5)]. In this work, we provide and analyze reference data for the He and Be atoms and the H₂ molecule. The short-range one-electron potentials required to keep the ground-density constant along a range-separated adiabatic connection [cf. Eq. (6)] are determined at the full configuration-interaction (FCI) level using Lieb’s Legendre-transform approach [61–63]. The excited-state energies of the long-range interacting Hamiltonian along the adiabatic connection [cf. Eq. (10)] are then calculated using the FCI method. Several accurate ground-state calculations have been performed in the past along the standard adiabatic connection [62–67] and range-separated adiabatic connections [1, 6, 67–69] for small atomic and molecular systems, but accurate calculations of excited-state energies along adiabatic connections are very scarce—see, however, Refs. 62, 70.

The remainder of this paper is organized as follows. In Section II, range-separated DFT is briefly reviewed and the definition of the excited states along the range-separated adiabatic connection is introduced. In Section III, the behaviour of the excited-state energies near the two endpoints of the adiabatic connection, the KS system and the physical system, is studied analytically. After giving computational details in Section IV, results along the full adiabatic-connection path are presented and discussed in Section V. Finally, some

concluding remarks are made in Section VI.

II. RANGE-SEPARATED DENSITY-FUNCTIONAL THEORY

In range-separated DFT (see, e.g., Ref. 1), the exact ground-state energy of an N -electron system is obtained by the following minimization over normalized multi-determinantal wave functions Ψ :

$$E_0 = \min_{\Psi} \left\{ \langle \Psi | \hat{T} + \hat{V}_{\text{ne}} + \hat{W}_{\text{ee}}^{\text{lr},\mu} | \Psi \rangle + \bar{E}_{\text{Hxc}}^{\text{sr},\mu}[n_{\Psi}] \right\}. \quad (1)$$

This expression contains the kinetic-energy operator \hat{T} , the nuclear–electron interaction operator $\hat{V}_{\text{ne}} = \int v_{\text{ne}}(\mathbf{r}) \hat{n}(\mathbf{r}) d\mathbf{r}$ expressed in terms of the density operator $\hat{n}(\mathbf{r})$, and a long-range (lr) electron–electron interaction operator

$$\hat{W}_{\text{ee}}^{\text{lr},\mu} = \frac{1}{2} \iint w_{\text{ee}}^{\text{lr},\mu}(r_{12}) \hat{n}_2(\mathbf{r}_1, \mathbf{r}_2) d\mathbf{r}_1 d\mathbf{r}_2, \quad (2)$$

expressed in terms of the pair-density operator $\hat{n}_2(\mathbf{r}_1, \mathbf{r}_2)$. In the present work, we use the error-function interaction

$$w_{\text{ee}}^{\text{lr},\mu}(r_{12}) = \frac{\text{erf}(\mu r_{12})}{r_{12}}, \quad (3)$$

where μ controls the range of the separation, with $1/\mu$ acting as a smooth cut-off radius. The corresponding complementary short-range (sr) Hartree–exchange–correlation density functional $\bar{E}_{\text{Hxc}}^{\text{sr},\mu}[n_{\Psi}]$ is evaluated at the density of Ψ : $n_{\Psi}(\mathbf{r}) = \langle \Psi | \hat{n}(\mathbf{r}) | \Psi \rangle$.

The Euler–Lagrange equation for the minimization of Eq. (1) leads to the (self-consistent) eigenvalue equation

$$\hat{H}^{\text{lr},\mu} |\Psi_0^{\mu}\rangle = \mathcal{E}_0^{\mu} |\Psi_0^{\mu}\rangle, \quad (4)$$

where Ψ_0^{μ} and \mathcal{E}_0^{μ} are the ground-state wave function and associated energy of the partially interacting Hamiltonian (with an explicit long-range electron–electron interaction)

$$\hat{H}^{\text{lr},\mu} = \hat{T} + \hat{V}_{\text{ne}} + \hat{W}_{\text{ee}}^{\text{lr},\mu} + \hat{V}_{\text{Hxc}}^{\text{sr},\mu}. \quad (5)$$

It contains the short-range Hartree–exchange–correlation potential operator, evaluated at the density $n_0(\mathbf{r}) = \langle \Psi_0^{\mu} | \hat{n}(\mathbf{r}) | \Psi_0^{\mu} \rangle$, which is equal to the ground-state density of the physical system for all μ ,

$$\hat{V}_{\text{Hxc}}^{\text{sr},\mu} = \int \bar{v}_{\text{Hxc}}^{\text{sr},\mu}[n_0](\mathbf{r}) \hat{n}(\mathbf{r}) d\mathbf{r}, \quad (6)$$

where

$$\bar{v}_{\text{Hxc}}^{\text{sr},\mu}[n](\mathbf{r}) = \frac{\delta \bar{E}_{\text{Hxc}}^{\text{sr},\mu}[n]}{\delta n(\mathbf{r})}. \quad (7)$$

For $\mu = 0$, $\hat{H}^{\text{lr},\mu}$ reduces to the standard non-interacting KS Hamiltonian, \hat{H}^{KS} , while for $\mu \rightarrow \infty$ it reduces to the physical Hamiltonian \hat{H} :

$$\hat{H}^{\text{KS}} = \hat{H}^{\text{lr},\mu=0} = \hat{T} + \hat{V}_{\text{ne}} + \hat{V}_{\text{Hxc}}, \quad (8)$$

$$\hat{H} = \hat{H}^{\text{lr},\mu=\infty} = \hat{T} + \hat{V}_{\text{ne}} + \hat{W}_{\text{ee}}. \quad (9)$$

Varying the parameter μ between these two limits, $\hat{H}^{\text{lr},\mu}$ defines a range-separated adiabatic connection, linking the non-interacting KS system to the physical system with the ground-state density kept constant (provided that the exact short-range Hartree–exchange–correlation potential $\hat{v}_{\text{Hxc}}^{\text{sr},\mu}(\mathbf{r})$ is used).

In this work we also consider the excited-state wave functions and energies of the long-range interacting Hamiltonian

$$\hat{H}^{\text{lr},\mu}|\Psi_k^\mu\rangle = \mathcal{E}_k^\mu|\Psi_k^\mu\rangle, \quad (10)$$

where $\hat{H}^{\text{lr},\mu}$ is Hamiltonian in Eq. (5), with the short-range Hartree–exchange–correlation potential evaluated at the *ground-state density* n_0 . In range-separated DFT, these excited-state wave functions and energies provide a natural first approximation to the excited-state wave functions and energies of the physical system. For $\mu = 0$, they reduce to the single-determinant eigenstates and associated energies of the non-interacting KS Hamiltonian,

$$\hat{H}^{\text{KS}}|\Phi_k^{\text{KS}}\rangle = \mathcal{E}_k^{\text{KS}}|\Phi_k^{\text{KS}}\rangle, \quad (11)$$

while, for $\mu \rightarrow \infty$, they reduce to the excited-state wave functions and energies of the physical Hamiltonian

$$\hat{H}|\Psi_k\rangle = E_k|\Psi_k\rangle. \quad (12)$$

We emphasize that, even with the exact (short-range) Hartree–exchange–correlation potential, the total energies $\mathcal{E}_k^{\text{KS}}$ (\mathcal{E}_k^μ) are not the exact energies of the physical system but the total energies of a non-interacting (partially interacting) fictitious system of electrons with Hamiltonian \hat{H}^{KS} ($\hat{H}^{\text{lr},\mu}$). Note also that, since the ionization energy is related to the asymptotic decay of the ground-state density, the ionization energy of the Hamiltonian in Eq. (10) is independent of μ and is equal to the ionization energy of the physical system. This is an appealing feature since it sets the correct energy window for bound excited states. Finally, note that the excitation energies $\Delta\mathcal{E}_k^\mu = \mathcal{E}_k^\mu - \mathcal{E}_0^\mu$ calculated from Eq. (10) constitute a starting point for range-separated linear-response theory based on the time-dependent generalization of Eq. (1) [52].

III. EXCITED-STATE ENERGIES NEAR THE KOHN–SHAM AND PHYSICAL SYSTEMS

In this section, we study analytically the behavior of the excited-state energies \mathcal{E}_k^μ as a function of the range-separation parameter μ close to the endpoints of the adiabatic connection: the KS system at $\mu = 0$ and the physical system at $\mu \rightarrow \infty$. This study will aid in the understanding of the numerical results presented in Section V.

A. Excited-state energies near the Kohn–Sham system

We first derive the expansion of the excited-state energies near $\mu = 0$, to see how the KS energies are affected by the introduction of the long-range electron–electron interaction. We assume that the system is spatially finite.

We rewrite the long-range interacting Hamiltonian of Eq. (5) as

$$\hat{H}^{\text{lr},\mu} = \hat{H}^{\text{KS}} + \hat{W}_{\text{ee}}^{\text{lr},\mu} - \hat{V}_{\text{Hxc}}^{\text{lr},\mu}, \quad (13)$$

with the long-range Hartree–exchange–correlation potential operator

$$\hat{V}_{\text{Hxc}}^{\text{lr},\mu} = \hat{V}_{\text{Hxc}} - \hat{V}_{\text{Hxc}}^{\text{sr},\mu} = \int v_{\text{Hxc}}^{\text{lr},\mu}(\mathbf{r})\hat{n}(\mathbf{r})\text{d}\mathbf{r}. \quad (14)$$

The expansion of the long-range two-electron interaction is straightforward [1] (valid for $\mu r_{12} \ll 1$)

$$\begin{aligned} w_{\text{ee}}^{\text{lr},\mu}(r_{12}) &= \frac{\text{erf}(\mu r_{12})}{r_{12}} \\ &= \frac{2\mu}{\sqrt{\pi}} + \mu^3 w_{\text{ee}}^{\text{lr},(3)}(r_{12}) + \mathcal{O}(\mu^5), \end{aligned} \quad (15)$$

with

$$w_{\text{ee}}^{\text{lr},(3)}(r_{12}) = -\frac{2}{3\sqrt{\pi}}r_{12}^2. \quad (16)$$

Note that the first term in the expansion of $w_{\text{ee}}^{\text{lr},\mu}(r_{12})$ in Eq. (15) is a spatial constant, $2\mu/\sqrt{\pi}$, which shows that what we call the long-range interaction does in fact contain also a contribution at short range [1]. Next, the expansion of the long-range Hartree–exchange–correlation potential

$$v_{\text{Hxc}}^{\text{lr},\mu}(\mathbf{r}) = \frac{\delta E_{\text{Hxc}}^{\text{lr},\mu}[n]}{\delta n(\mathbf{r})} \quad (17)$$

can be determined from the expansion of the corresponding energy functional $E_{\text{Hxc}}^{\text{lr},\mu}[n]$. As derived in Ref. 1, the expansion of the Hartree–exchange

part begins at first order and may be written as

$$E_{\text{Hxc}}^{\text{lr},\mu}[n] = \frac{\mu}{\sqrt{\pi}} \iint n_2^{\text{KS}}(\mathbf{r}_1, \mathbf{r}_2) d\mathbf{r}_1 d\mathbf{r}_2 + \frac{\mu^3}{2} \iint n_2^{\text{KS}}(\mathbf{r}_1, \mathbf{r}_2) w_{\text{ee}}^{\text{lr},(3)}(r_{12}) d\mathbf{r}_1 d\mathbf{r}_2 + \mathcal{O}(\mu^5). \quad (18)$$

where $n_2^{\text{KS}}(\mathbf{r}_1, \mathbf{r}_2)$ is the KS pair density, while the expansion of the correlation part only begins at sixth order (assuming a non-degenerate KS ground state)

$$E_c^{\text{lr},\mu}[n] = 0 + \mathcal{O}(\mu^6). \quad (19)$$

If the functional derivative of $E_{\text{Hxc}}^{\text{lr},\mu}[n]$ is taken with respect to density variations that preserve the number of electrons, $\int \delta n(\mathbf{r}) d\mathbf{r} = 0$, then the first-order term in Eq. (18) does not contribute due to the fixed normalization of the KS pair density, $\iint n_2^{\text{KS}}(\mathbf{r}_1, \mathbf{r}_2) d\mathbf{r}_1 d\mathbf{r}_2 = N(N-1)$. The derivative is then defined up to an additive (μ -dependent) constant C^μ , which can be fixed by requiring that a distant electron experiences zero potential interaction in Eq. (13), amounting to setting the zero-energy reference. The linear term in μ in the long-range Hartree–exchange–correlation potential can then be determined as follows.

To first order in μ , the long-range electron–electron interaction tends to a constant, $2\mu/\sqrt{\pi}$. A distant electron (with $1 \ll r_{12} \ll 1/\mu$) then experiences a constant interaction $2(N-1)\mu/\sqrt{\pi}$ with the remaining $N-1$ other electrons. This constant must be exactly compensated by the long-range Hartree–exchange–correlation potential in Eq. (13), so that its first-order term in μ must also be $2(N-1)\mu/\sqrt{\pi}$. The expansion of $v_{\text{Hxc}}^{\text{lr},\mu}(\mathbf{r})$ therefore takes the form

$$v_{\text{Hxc}}^{\text{lr},\mu}(\mathbf{r}) = \frac{2(N-1)\mu}{\sqrt{\pi}} + \mu^3 v_{\text{Hxc}}^{\text{lr},(3)}(\mathbf{r}) + \mathcal{O}(\mu^5), \quad (20)$$

where $v_{\text{Hxc}}^{\text{lr},(3)}(\mathbf{r})$ is the third-order contribution.

Combining Eqs. (15) and (20), we arrive at the following expansion of the long-range interacting Hamiltonian of Eq. (13):

$$\hat{H}^{\text{lr},\mu} = \hat{H}^{\text{KS}} + \mu \hat{H}^{\text{lr},(1)} + \mu^3 \hat{H}^{\text{lr},(3)} + \mathcal{O}(\mu^5), \quad (21)$$

with a constant first-order correction

$$\hat{H}^{\text{lr},(1)} = -\frac{N(N-1)}{\sqrt{\pi}} \quad (22)$$

and the following third-order correction

$$\hat{H}^{\text{lr},(3)} = \hat{W}_{\text{ee}}^{\text{lr},(3)} - \hat{V}_{\text{Hxc}}^{\text{lr},(3)}, \quad (23)$$

$$\hat{W}_{\text{ee}}^{\text{lr},(3)} = \frac{1}{2} \iint w_{\text{ee}}^{\text{lr},(3)}(r_{12}) \hat{n}_2(\mathbf{r}_1, \mathbf{r}_2) d\mathbf{r}_1 d\mathbf{r}_2, \quad (24)$$

$$\hat{V}_{\text{Hxc}}^{\text{lr},(3)} = \int v_{\text{Hxc}}^{\text{lr},(3)}(\mathbf{r}) \hat{n}(\mathbf{r}) d\mathbf{r}. \quad (25)$$

Since the first-order correction in the Hamiltonian is a constant, it does not affect the associated wave functions. The expansion of the wave functions therefore begins at third order in μ :

$$\Psi_k^\mu = \Phi_k^{\text{KS}} + \mu^3 \Psi_k^{(3)} + \mathcal{O}(\mu^5). \quad (26)$$

Using normalized KS wave functions $\langle \Phi_k^{\text{KS}} | \Phi_k^{\text{KS}} \rangle = 1$, the expansion of the total energy for the state k is then

$$\mathcal{E}_k^\mu = \mathcal{E}_k^{\text{KS}} - \frac{N(N-1)}{\sqrt{\pi}} \mu + \mu^3 \langle \Phi_k^{\text{KS}} | \hat{H}^{\text{lr},(3)} | \Phi_k^{\text{KS}} \rangle + \mathcal{O}(\mu^5). \quad (27)$$

The first-order contribution is the same for all states, cancelling out in the differences between the energies of two states. As a result, the corrections to the KS excitation energies are third order in μ .

For closed shells, the expansion of the difference between the singlet and triplet energies associated with the single excitation $i \rightarrow a$ can be obtained by applying Eq. (27) with the spin-adapted KS wave functions ${}^1\Phi_k^{\text{KS}} = (\Phi_{i \rightarrow a}^{\text{KS}} + \Phi_{i \rightarrow \bar{a}}^{\text{KS}})/\sqrt{2}$, for the singlet state, and ${}^{3,1}\Phi_k^{\text{KS}} = \Phi_{i \rightarrow a}^{\text{KS}}$, for the triplet state with spin projection $M_S = 1$. Only the two-electron term then contributes:

$$\begin{aligned} \Delta \mathcal{E}_{i \rightarrow a}^{\mu,1-3} &= 2\mu^3 \langle ia | \hat{w}_{\text{ee}}^{\text{lr},(3)} | ai \rangle + \mathcal{O}(\mu^5) \\ &= \frac{8\mu^3}{3\sqrt{\pi}} |\langle i | \hat{\mathbf{r}} | a \rangle|^2 + \mathcal{O}(\mu^5), \end{aligned} \quad (28)$$

where we have used $r_{12}^2 = r_1^2 + r_2^2 - 2\mathbf{r}_1 \cdot \mathbf{r}_2$. The appearance of the transition dipole moment integral in Eq. (28) means that, for an atomic system, the singlet–triplet energy splitting appears at third order in μ if the difference between the angular momentum of the orbitals φ_i and φ_a is $\Delta\ell = +1$ or -1 . Otherwise, the splitting appears at a higher order in μ .

B. Excited-state energies near the physical system

We now derive the asymptotic expansion of the excited-state energies when $\mu \rightarrow \infty$, which shows how the exact excited-state energies are affected by the removal of the very short-range part of the electron–electron interaction.

For this purpose, we rewrite the long-range interacting Hamiltonian of Eq. (5) as

$$\hat{H}^{\text{lr},\mu} = \hat{H} - \hat{W}_{\text{ee}}^{\text{sr},\mu} + \hat{V}_{\text{Hxc}}^{\text{sr},\mu}, \quad (29)$$

where \hat{H} is the Hamiltonian of the physical system,

$$\hat{W}_{\text{ee}}^{\text{sr},\mu} = \frac{1}{2} \iint w_{\text{ee}}^{\text{sr},\mu}(r_{12}) \hat{n}_2(\mathbf{r}_1, \mathbf{r}_2) d\mathbf{r}_1 d\mathbf{r}_2 \quad (30)$$

is the short-range electron–electron interaction operator defined with the complementary error-function interaction

$$w_{\text{ee}}^{\text{sr},\mu}(r_{12}) = \frac{\text{erfc}(\mu r_{12})}{r_{12}}, \quad (31)$$

and $\hat{V}_{\text{Hxc}}^{\text{sr},\mu}$ is the short-range Hartree–exchange–correlation potential operator in Eq. (6). The first term in the asymptotic expansion of $w_{\text{ee}}^{\text{sr},\mu}(r_{12})$ can be written in terms of a delta function [1] (valid for $\mu r_{12} \gg 1$)

$$w_{\text{ee}}^{\text{sr},\mu}(r_{12}) = \frac{\pi}{\mu^2} \delta(\mathbf{r}_{12}) + \mathcal{O}\left(\frac{1}{\mu^3}\right), \quad (32)$$

while the expansion of $\bar{v}_{\text{Hxc}}^{\text{sr},\mu}(\mathbf{r}) = \delta \bar{E}_{\text{Hxc}}^{\text{sr},\mu}[n]/\delta n(\mathbf{r})$ can be obtained from that of $\bar{E}_{\text{Hxc}}^{\text{sr},\mu}[n]$. As derived in Ref. 1, the expansion of the long-range Hartree–exchange energy is

$$E_{\text{Hx}}^{\text{sr},\mu}[n] = \frac{\pi}{2\mu^2} \int n_2^{\text{KS}}(\mathbf{r}, \mathbf{r}) \text{d}\mathbf{r} + \mathcal{O}\left(\frac{1}{\mu^4}\right), \quad (33)$$

where $n_2^{\text{KS}}(\mathbf{r}, \mathbf{r})$ is the KS on-top pair density, while the expansion of the long-range correlation energy is

$$\bar{E}_c^{\text{sr},\mu}[n] = \frac{\pi}{2\mu^2} \int n_{2,c}(\mathbf{r}, \mathbf{r}) \text{d}\mathbf{r} + \mathcal{O}\left(\frac{1}{\mu^3}\right), \quad (34)$$

where $n_{2,c}(\mathbf{r}, \mathbf{r})$ is the on-top correlation pair density of the physical system. Therefore, the expansion of the short-range Hartree–exchange–correlation potential takes the form

$$\bar{v}_{\text{Hxc}}^{\text{sr},\mu}(\mathbf{r}) = \frac{1}{\mu^2} \bar{v}_{\text{Hxc}}^{\text{sr},(-2)}(\mathbf{r}) + \mathcal{O}\left(\frac{1}{\mu^3}\right), \quad (35)$$

where $\bar{v}_{\text{Hxc}}^{\text{sr},(-2)}(\mathbf{r})$ is the μ^{-2} contribution formally obtained by taking the functional derivative of Eqs. (33) and (34).

Substituting Eqs. (32) and (35) into Eq. (29), we obtain the asymptotic expansion of the long-range interacting Hamiltonian as

$$\hat{H}^{\text{lr},\mu} = \hat{H} + \frac{1}{\mu^2} \hat{H}^{\text{lr},(-2)} + \mathcal{O}\left(\frac{1}{\mu^3}\right), \quad (36)$$

where $\hat{H}^{\text{lr},(-2)} = -\hat{W}_{\text{ee}}^{\text{sr},(-2)} + \hat{V}_{\text{Hxc}}^{\text{sr},(-2)}$ is composed of an on-top two-electron term and a one-electron term:

$$\hat{W}_{\text{ee}}^{\text{sr},(-2)} = \frac{\pi}{2} \int \hat{n}_2(\mathbf{r}, \mathbf{r}) \text{d}\mathbf{r}, \quad (37)$$

$$\hat{V}_{\text{Hxc}}^{\text{sr},(-2)} = \int \bar{v}_{\text{Hxc}}^{\text{sr},(-2)}(\mathbf{r}) \hat{n}(\mathbf{r}) \text{d}\mathbf{r}. \quad (38)$$

The expansion of the Hamiltonian in Eq. (36) suggests a similar expansion for the excited-state wave

functions, $\Psi_k^\mu = \Psi_k + \mu^{-2} \Psi_k^{(-2)} + \mathcal{O}(\mu^{-3})$. However, as shown in Ref. 71, this expansion is not valid for $r_{12} \ll 1/\mu$. The contribution of the wave function for small r_{12} to the integral for the total energy $\mathcal{E}_k^\mu = \langle \Psi_k^\mu | \hat{H}^{\text{lr},\mu} | \Psi_k^\mu \rangle$ nevertheless vanishes in the limit $\mu \rightarrow \infty$, and the asymptotic expansion of the total energy of the state k is

$$\mathcal{E}_k^\mu = E_k + \frac{1}{\mu^2} \langle \Psi_k | \hat{H}^{\text{lr},(-2)} | \Psi_k \rangle + \mathcal{O}\left(\frac{1}{\mu^3}\right), \quad (39)$$

where the wave function Ψ_k is normalized to unity.

IV. COMPUTATIONAL DETAILS

Calculations have been performed for the He and Be atoms and for the H₂ molecule with a development version of the DALTON program [72, 73], using the implementation described in Refs. 63 and 69. First, a FCI calculation was performed to determine the exact ground-state density within the basis set considered, followed by a Lieb optimization [62] of the short-range potential $v^{\text{sr},\mu}(\mathbf{r}) = v_{\text{ne}}(\mathbf{r}) + \bar{v}_{\text{Hxc}}^{\text{sr},\mu}(\mathbf{r})$ also at the FCI level to reproduce the FCI ground-state density in the presence of the long-range electron–electron interaction $w_{\text{ee}}^{\text{lr},\mu}(r_{12})$. The FCI excited-state energies were then calculated using the partially interacting Hamiltonian with the interaction $w_{\text{ee}}^{\text{lr},\mu}(r_{12})$ and effective potential $v^{\text{sr},\mu}(\mathbf{r})$.

The Lieb maximization was performed using the short-range analogue of the algorithm of Wu and Yang [74], in which the potential is expanded as

$$v^{\text{sr},\mu}(\mathbf{r}) = v_{\text{ne}}(\mathbf{r}) + v_{\text{ref}}^{\text{sr},\mu}(\mathbf{r}) + \sum_t b_t g_t(\mathbf{r}). \quad (40)$$

where the reference potential is the short-range analogue of the Fermi–Amaldi potential

$$v_{\text{ref}}^{\text{sr},\mu}(\mathbf{r}) = \frac{N-1}{N} \int n_0(\mathbf{r}') w_{\text{ee}}^{\text{sr}}(|\mathbf{r} - \mathbf{r}'|) \text{d}\mathbf{r}', \quad (41)$$

calculated for a fixed N -electron density n_0 , to ensure the correct asymptotic behaviour. The same Gaussian basis set $\{g_t\}$ is used for the expansion of the potential and the molecular orbitals. The coefficients b_t are optimized by the Newton method, using a regularized Hessian with a truncated singular-value-decomposition cutoff of 10^{-7} for He and 10^{-6} for Be and H₂.

Even-tempered Kaufmann basis sets [75] and uncontracted correlation consistent Dunning basis sets [76] augmented with diffuse functions were tested extensively for the He atom, especially to converge the lowest P state. No significant differences were observed using the two basis sets and

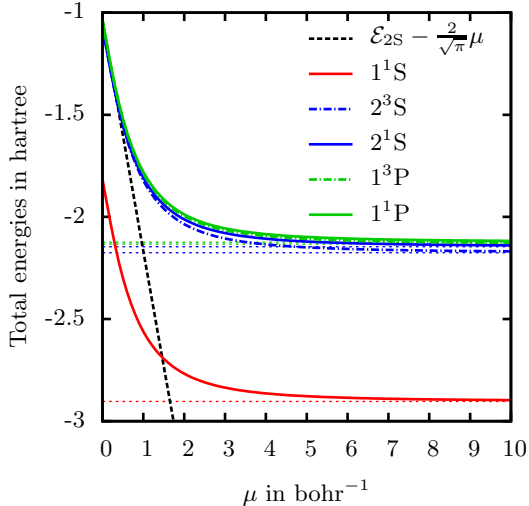


Figure 1: Ground- and excited-state total energies \mathcal{E}_k^μ (in hartree) of the He atom as a function of μ (in bohr $^{-1}$). The total energies of the physical system $E_k = \mathcal{E}_k^{\mu \rightarrow \infty}$ are plotted as horizontal dotted lines. The slope at $\mu = 0$ is shown by the black dashed line for the first excited state.

only the Dunning basis sets are used in the following. The basis sets used are: uncontracted t-aug-cc-pV5Z for He, uncontracted d-aug-cc-pVDZ for Be, and uncontracted d-aug-cc-pVTZ Dunning basis sets for H₂.

Calculations were performed for about 30 values of μ between 0 to 10 bohr $^{-1}$ (with about half the points between 0 and 1 where the energies vary the most). Cubic spline interpolation has been used on this calculated data when plotting the total and excitation energies as a function of μ . For later use, analytical expressions were also fitted to the calculated total energies and excitation energies. The forms used in the fitting were chosen to satisfy the expansions at small and large μ values as presented in Eqs. (27) and (39). The details of these fits are given in the supplementary material [77].

V. RESULTS AND DISCUSSION

A. Helium atom

The total energies of the ground state 1^1S and of the first Rydberg-like singlet and triplet S and P excited states of the He atom are plotted as a function of the range-separation parameter μ in Figure 1. At $\mu = 0$, the KS non-interacting total energies are obtained. Being sums of orbital energies with a resulting double counting of electron repulsion, these quantities are well above the

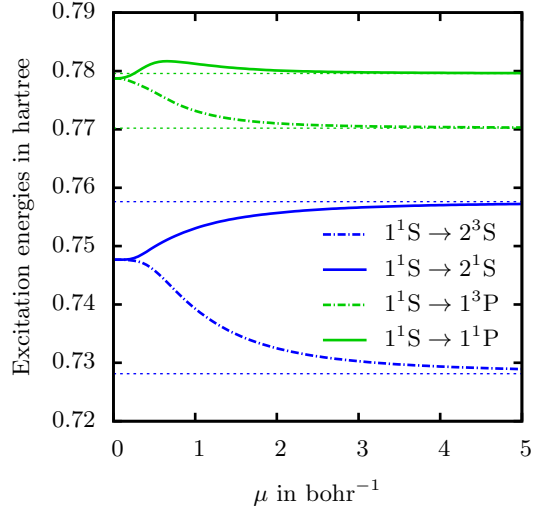


Figure 2: Excitation energies $\Delta\mathcal{E}_k^\mu = \mathcal{E}_k^\mu - \mathcal{E}_0^\mu$ (in hartree) of the He atom as a function of μ (in bohr $^{-1}$). The excitation energies of the physical system $\Delta E_k = \Delta\mathcal{E}_k^{\mu \rightarrow \infty}$ are plotted as horizontal dotted lines.

total energies of the physical system (higher by about 1 hartree). When the long-range electron–electron interaction is added by increasing μ from $\mu = 0$, the total energies decrease linearly with μ with a slope of $-2/\sqrt{\pi}$, in accordance with the linear term in the expansion of Eq. (27) for $N = 2$. For larger μ values, the total energy curves flatten and approach the energies of the physical system asymptotically as $1/\mu^2$ as $\mu \rightarrow \infty$, in accordance with Eq. (39). The total energies along the adiabatic connection are poor approximations to the total energies of the physical system unless the range-separation parameter μ is large. Specifically, $\mu \gtrsim 6$ is required to be within 10 mhartree of the exact total energies.

The lowest singlet and triplet excitation energies are plotted in Figure 2. The KS singlet and triplet excitation energies are degenerate and, as already observed for a few atomic systems in Refs. 78–80, are bracketed by the singlet and triplet excitation energies of the physical system. As μ increases from $\mu = 0$, the excitation energies vary as μ^3 since the linear term in Eq. (27) cancels out for energy differences. The singlet–triplet degeneracy is lifted and the excitation energies converge to the exact singlet and triplet excitation energies when $\mu \rightarrow \infty$. Whereas a monotonic variation of the excitation energy with μ can be observed for the singlet and triplet $1\text{S} \rightarrow 2\text{S}$ excitations and for the triplet $1^1\text{S} \rightarrow 1^3\text{P}$ excitation, a non-monotonic variation is observed for the singlet $1^1\text{S} \rightarrow 1^1\text{P}$ excitation. This behaviour could be an artefact of the basis-set expansions (either orbital or potential), noting that a similar behaviour was ob-

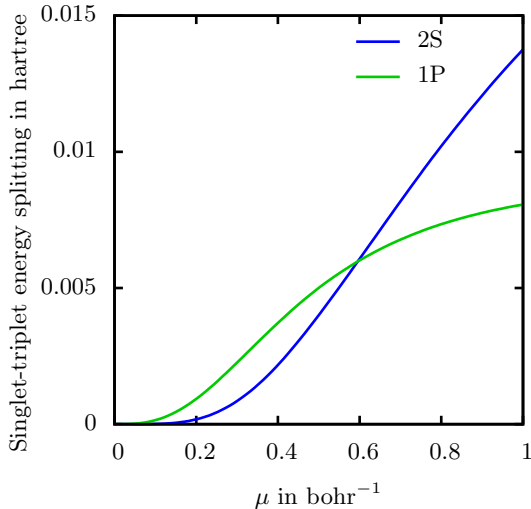


Figure 3: Singlet–triplet energy splittings (in hartree) for the He atom as a function of μ (in bohr⁻¹).

served for other excitations in a smaller basis set and was removed by enlarging the basis set (the basis set dependence of the singlet $1^1S \rightarrow 1^1P$ excitation energy is given in the supplementary material [77]). In line with previous observations in Refs. [78, 80] for the KS system, the excitation energies for Rydberg-type states along the adiabatic connection are rather good approximations to the excitation energies of the physical system (the maximal error is about 0.02 hartree at $\mu = 0$ for the triplet $1^1S \rightarrow 2^3S$ excitation), becoming better and better for high-lying states as they must eventually converge to the exact ionization energy.

The singlet–triplet energy splittings for the 2S and 1P states are plotted in Figure 3. The expansion at small μ of Eq. (28) predicts the singlet–triplet splitting to increase as μ^3 for the 1P state since it corresponds to the $1s \rightarrow 2p$ excitation in the KS system, so that $\Delta\ell = 1$. By contrast, the singlet–triplet splitting should increase at most as μ^5 for the 2S state since it corresponds to the $1s \rightarrow 2s$ excitation in the KS system, so that $\Delta\ell = 0$. This difference is clearly visible in Figure 3, where the 2S curve for the singlet–triplet splitting initially increases more slowly than the 1P curve.

B. Beryllium atom

The total energies of the ground state 1^1S and of the valence singlet and triplet 1P excited states of the Be atom are plotted in Figure 4. The KS total energies are approximately 6 hartree above the physical energies. At small μ , an initial slope of $-12/\sqrt{\pi}$ is observed for all states, in accordance

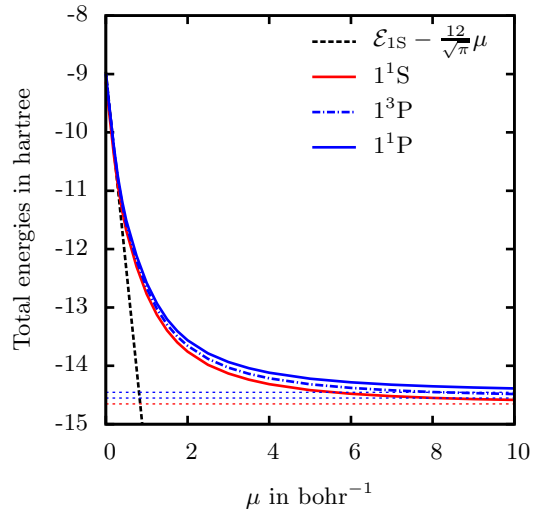


Figure 4: Ground- and excited-state total energies \mathcal{E}_k^μ (in hartree) of the Be atom as a function of μ (in bohr⁻¹). The total energies of the physical system $E_k = \mathcal{E}_k^{\mu \rightarrow \infty}$ are plotted as horizontal dotted lines. The slope at $\mu = 0$ is shown in dashed line.

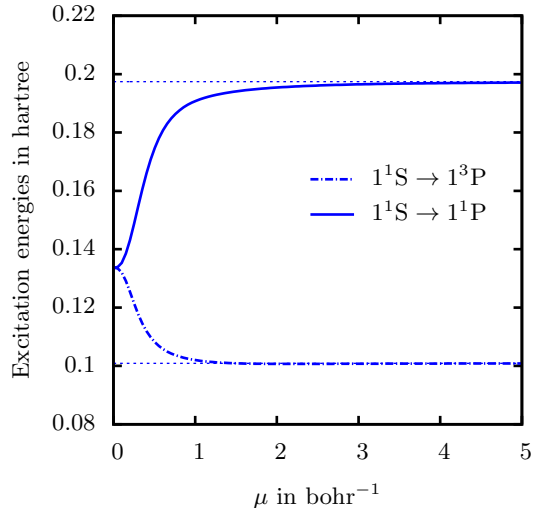


Figure 5: Excitation energies $\Delta\mathcal{E}_k^\mu = \mathcal{E}_k^\mu - \mathcal{E}_0^\mu$ (in hartree) of the Be atom as a function of μ (in bohr⁻¹). The excitation energies of the physical system $\Delta E_k = \Delta\mathcal{E}_k^{\mu \rightarrow \infty}$ are plotted as horizontal dotted lines.

with Eq. (27) with $N = 4$. However, convergence to the physical energies with increasing μ is much slower than for the He atom, owing to the short inter-electronic distances in the Be $1s$ core region, which are consequently probed at larger μ values.

The singlet and triplet excitation energies are plotted in Figure 5. As for He, the KS excitation energies are bracketed by the singlet and triplet excitation energies of the physical system. Not

surprisingly, the KS excitation energies are poorer approximations to the exact excitation energies for these valence excitations in Be than for the Rydberg excitations in He. As μ increases, the KS excitation energies rapidly converge to the physical excitation energies. Clearly, the slow convergence of the core energies does not affect the convergence of the valence excitation energies.

Close to the KS system, at $\mu = 0$, the excitation energies are quite sensitive to the introduction of a small portion of electron–electron interaction in the Hamiltonian, which may be interpreted as a sign of static correlation. For $\mu \approx 0.4 - 0.5$, a typical μ value in range-separated DFT calculations [18, 81], the calculated excitation energies are significantly better approximations to the exact excitation energies than are the KS excitation energies. This observation justifies range-separated multi-determinantal linear-response DFT calculations, which take these excitation energies as a starting point.

C. Hydrogen molecule

The first few excitation energies of H_2 at the equilibrium bond distance are plotted against μ in Figure 6. As for the atoms, the valence excitations energies vary much more along the adiabatic connection than do the Rydberg-like excitation energies. Note also that the energetic ordering of the states changes along the adiabatic connection. With our choice of basis set, we also observe that the higher singlet excitation energies do not depend monotonically on μ , approaching the physical limits from above, as observed for He. Again, the excitation energies around $\mu \approx 0.4 - 0.5$ represent better approximations to the exact excitation energies than the KS excitation energies.

Finally, we consider the interesting case of the dissociation of the H_2 molecule. The first excitation energies at three times the equilibrium distance are shown in Figure 7. With increasing bond distance, the $1\sigma_g$ and $1\sigma_u$ molecular orbitals become degenerate. Consequently, the KS excitation energy for the single excitation $1\sigma_g \rightarrow 1\sigma_u$ goes to zero. Moreover, the KS excitation energy for the double excitation $(1\sigma_g)^2 \rightarrow (1\sigma_u)^2$ also goes to zero (albeit more slowly). This behaviour is in contrast to that of the physical system, where only the excitation energy to the triplet $1^3\Sigma_u^+$ state goes to zero, whilst those to the singlet $1^1\Sigma_u^+$ state and the $2^1\Sigma_g^+$ state (the latter connected to the double excitation in the KS system) go to finite values.

Clearly, the excitation energies of KS theory are poor approximations to the exact excitation energies, making it difficult to recover from these poor starting values in practical linear-response

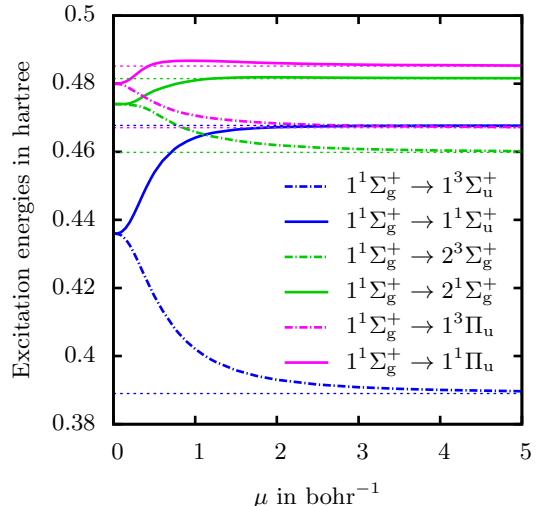


Figure 6: Excitation energies $\Delta\mathcal{E}_k^\mu = \mathcal{E}_k^\mu - \mathcal{E}_0^\mu$ (in hartree) of the H_2 molecule at the equilibrium internuclear distance as a function of μ (in bohr⁻¹). The excitation energies of the physical system $\Delta E_k = \Delta\mathcal{E}_k^{\mu \rightarrow \infty}$ are plotted as horizontal dotted lines.

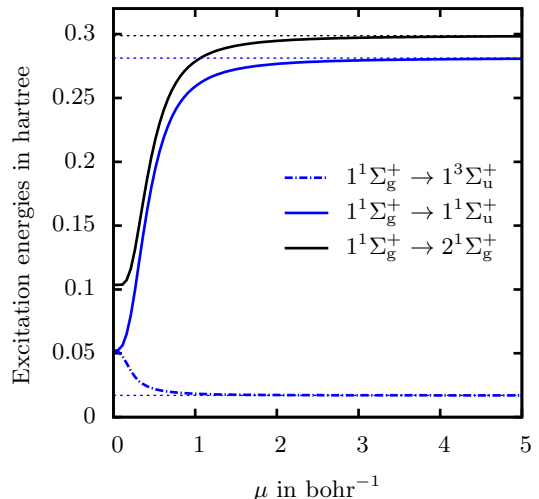


Figure 7: Excitation energies $\Delta\mathcal{E}_k^\mu = \mathcal{E}_k^\mu - \mathcal{E}_0^\mu$ (in hartree) of the H_2 molecule at 3 times the equilibrium internuclear distance as a function of μ (in bohr⁻¹). The excitation energies of the physical system $\Delta E_k = \Delta\mathcal{E}_k^{\mu \rightarrow \infty}$ are plotted as horizontal dotted lines.

TDDFT calculations. As μ increases from $\mu = 0$, the excitation energies to the singlet $1^1\Sigma_u^+$ and $2^1\Sigma_g^+$ states vary abruptly, rapidly approaching the physical values. This sensitivity to the inclusion of the electron–electron interaction is a clear signature of strong static correlation effects, emphasizing the importance of a multi-determinantal description in such situations. At $\mu \approx 0.4 - 0.5$, the

$1^1\Sigma_u^+$ and $2^1\Sigma_g^+$ excitation energies, although still too low, are much better approximations than the KS excitation energies, constituting a strong motivation for range-separated multi-determinantal approaches in linear-response theory.

VI. CONCLUSIONS

We have studied the variation of total energies and excitation energies along a range-separated adiabatic connection, linking the non-interacting KS system ($\mu = 0$) to the physical system ($\mu \rightarrow \infty$) by progressively switching on the long-range part of the electron–electron interaction with the range-separation parameter μ , whilst keeping the ground-state density constant. This behaviour is of interest for the development and analysis of range-separated DFT schemes for the calculation of excitation energies, such as the linear-response range-separated schemes of Refs. 52, 53, 55.

Reference calculations were performed for the He and Be atoms and the H₂ molecule. Except when μ is large, the ground- and excited-state total energies along the adiabatic connection are poor approximations to the corresponding energies of the physical system. On the other hand, the excitation energies are good approximations to the excitation energies of the physical system for most of the adiabatic connection curve, except close to the KS system ($\mu = 0$). In particular, the excitation energies obtained at $\mu \approx 0.4 - 0.5$, typically used in range-separated DFT calculations, are significantly better approximations to the exact excitation energies than are the KS excitation energies. This behaviour appears to be particularly evident for situations involving strong static correlation effects and double excitations, as observed for the dissociating H₂ molecule.

These observations suggest that the excitation energies of the long-range interacting Hamiltonian

in range-separated DFT may be useful as first estimates of the excitation energies of the physical system. However, if one cannot afford to use large μ values ($\mu > 2 - 3$), these excitation energies should be considered only as starting approximations, suitable for correction by, for example, linear-response range-separated theory.

In future work, we will utilize the present reference data to assess the approximations made in practical linear-response range-separated schemes, where the long-range contribution is treated, for example, at the Hartree–Fock, MCSCF or SOPPA levels of theory, while the short-range part is described by semi-local density-functional approximations. We will also use the results of this work to guide the development of time-independent range-separated DFT methods for the calculation of excitation energies as alternatives to linear-response schemes—in particular, for methods based on perturbation theories [79, 82] or extrapolations [83, 84] along the adiabatic connection.

Acknowledgments

E. R. and J. T. gratefully acknowledge the hospitality of the Centre for Theoretical and Computational Chemistry (CTCC), University of Oslo, where part of this research was done. E. R. also thanks A. Borgoo and S. Kvaal for helpful discussions. T. H. acknowledges support from the Norwegian Research Council through the CoE Centre for Theoretical and Computational Chemistry (CTCC) Grant No. 179568/V30 and the Grant No. 171185/V30 and through the European Research Council under the European Union Seventh Framework Program through the Advanced Grant ABACUS, ERC Grant Agreement No. 267683. A. M. T. is grateful for support from the Royal Society University Research Fellowship scheme.

-
- [1] J. Toulouse, F. Colonna, and A. Savin, Phys. Rev. A **70**, 062505 (2004).
 - [2] P. Hohenberg and W. Kohn, Phys. Rev. **136**, B 864 (1964).
 - [3] W. Kohn and L. J. Sham, Phys. Rev. **140**, A1133 (1965).
 - [4] A. Savin, in *Recent Dev. Mod. Density Funct. Theory*, edited by J. M. Seminario (Elsevier, Amsterdam, 1996), pp. 327–357.
 - [5] W. Yang, J. Chem. Phys. **109**, 10107 (1998).
 - [6] R. Pollet, F. Colonna, T. Leininger, H. Stoll, H.-J. Werner, and A. Savin, Int. J. Quantum. Chem. **91**, 84 (2003).
 - [7] A. Savin, F. Colonna, and R. Pollet, Int. J. Quantum. Chem. **93**, 166 (2003).
 - [8] J. Toulouse, A. Savin, and H.-J. Flad, Int. J. Quantum Chem. **100**, 1047 (2004).
 - [9] J. Toulouse, F. Colonna, and A. Savin, J. Chem. Phys. **122**, 014110 (2005).
 - [10] J. Toulouse, P. Gori-Giorgi, and A. Savin, Theor. Chem. Acc. **114**, 305 (2005).
 - [11] E. Goll, H.-J. Werner, and H. Stoll, Phys. Chem. Chem. Phys. **7**, 3917 (2005).
 - [12] S. Paziani, S. Moroni, P. Gori-Giorgi, and G. B. Bachelet, Phys. Rev. B **73**, 155111 (2006).
 - [13] E. Goll, M. Ernst, F. Moegle-Hofacker, and H. Stoll, J. Chem. Phys. **130**, 234112 (2009).
 - [14] A. Savin and H.-J. Flad, Int. J. Quantum. Chem.

- 56**, 327 (1995).
- [15] A. Savin, in *Recent Adv. Density Funct. Theory*, edited by D. P. Chong (World Scientific, 1996).
- [16] T. Leininger, H. Stoll, H.-J. Werner, and A. Savin, *Chem. Phys. Lett.* **275**, 151 (1997).
- [17] R. Pollet, A. Savin, T. Leininger, and H. Stoll, *J. Chem. Phys.* **116**, 1250 (2002).
- [18] E. Fromager, J. Toulouse, and H. J. A. Jensen, *J. Chem. Phys.* **126**, 74111 (2007).
- [19] E. Fromager, F. Réal, P. Wählin, U. Wahlgren, and H. J. A. Jensen, *J. Chem. Phys.* **131**, 054107 (2009).
- [20] A. Stoyanova, A. M. Teale, J. Toulouse, T. Helgaker, and E. Fromager, *J. Chem. Phys.* **139**, 134113 (2013).
- [21] K. Pernal, *Phys. Rev. A* **81**, 52511 (2010).
- [22] D. R. Rohr, J. Toulouse, and K. Pernal, *Phys. Rev. A* **82**, 52502 (2010).
- [23] D. R. Rohr and K. Pernal, *J. Chem. Phys.* **135**, 74104 (2011).
- [24] T. Tsuchimochi, G. E. Scuseria, and A. Savin, *J. Chem. Phys.* **132**, 24111 (2010).
- [25] T. Tsuchimochi and G. E. Scuseria, *J. Chem. Phys.* **134**, 64101 (2011).
- [26] J. G. Ángyán, I. C. Gerber, A. Savin, and J. Toulouse, *Phys. Rev. A* **72**, 12510 (2005).
- [27] I. C. Gerber and J. G. Ángyán, *Chem. Phys. Lett.* **416**, 370 (2005).
- [28] I. C. Gerber and J. G. Ángyán, *J. Chem. Phys.* **126**, 44103 (2007).
- [29] J. G. Ángyán, *Phys. Rev. A* **78**, 22510 (2008).
- [30] E. Fromager and H. J. A. Jensen, *Phys. Rev. A* **78**, 22504 (2008).
- [31] E. Goll, T. Leininger, F. R. Manby, A. Mitrushchenkov, H.-J. Werner, and H. Stoll, *Phys. Chem. Chem. Phys.* **10**, 3353 (2008).
- [32] B. G. Janesko and G. E. Scuseria, *Phys. Chem. Chem. Phys.* **11**, 9677 (2009).
- [33] E. Fromager, R. Cimiraglia, and H. J. A. Jensen, *Phys. Rev. A* **81**, 24502 (2010).
- [34] S. Chabbal, H. Stoll, H.-J. Werner, and T. Leininger, *Mol. Phys.* **108**, 3373 (2010).
- [35] S. Chabbal, D. Jacquemin, C. Adamo, H. Stoll, and T. Leininger, *J. Chem. Phys.* **133**, 151104 (2010).
- [36] E. Fromager and H. J. A. Jensen, *J. Chem. Phys.* **135**, 034116 (2011).
- [37] Y. Cornaton, A. Stoyanova, H. J. A. Jensen, and E. Fromager, *Phys. Rev. A* **88**, 022516 (2013).
- [38] E. Goll, H.-J. Werner, H. Stoll, T. Leininger, P. Gori-Giorgi, and A. Savin, *Chem. Phys.* **329**, 276 (2006).
- [39] E. Goll, H. Stoll, C. Thierfelder, and P. Schwerdtfeger, *Phys. Rev. A* **76**, 32507 (2007).
- [40] E. Goll, H.-J. Werner, and H. Stoll, *Chem. Phys.* **346**, 257 (2008).
- [41] J. Toulouse, I. C. Gerber, G. Jansen, A. Savin, and J. G. Ángyán, *Phys. Rev. Lett.* **102**, 96404 (2009).
- [42] B. G. Janesko, T. M. Henderson, and G. E. Scuseria, *J. Chem. Phys.* **130**, 81105 (2009).
- [43] B. G. Janesko, T. M. Henderson, and G. E. Scuseria, *J. Chem. Phys.* **131**, 34110 (2009).
- [44] B. G. Janesko and G. E. Scuseria, *J. Chem. Phys.* **131**, 154106 (2009).
- [45] W. Zhu, J. Toulouse, A. Savin, and J. G. Ángyán, *J. Chem. Phys.* **132**, 244108 (2010).
- [46] J. Toulouse, W. Zhu, J. G. Ángyán, and A. Savin, *Phys. Rev. A* **82**, 32502 (2010).
- [47] J. Paier, B. G. Janesko, T. M. Henderson, G. E. Scuseria, A. Grüneis, and G. Kresse, *J. Chem. Phys.* **132**, 094103 (2010).
- [48] J. Toulouse, W. Zhu, A. Savin, G. Jansen, and J. G. Ángyán, *J. Chem. Phys.* **135**, 084119 (2011).
- [49] J. G. Ángyán, R.-F. Liu, J. Toulouse, and G. Jansen, *J. Chem. Theory Comput.* **7**, 3116 (2011).
- [50] R. M. Ireland, T. M. Henderson, and G. E. Scuseria, *J. Chem. Phys.* **135**, 94105 (2011).
- [51] T. Gould and J. F. Dobson, *Phys. Rev. B* **84**, 241108 (2011).
- [52] E. Fromager, S. Knecht, and H. J. A. Jensen, *J. Chem. Phys.* **138**, 084101 (2013).
- [53] E. Rebolini, A. Savin, and J. Toulouse, *Mol. Phys.* **111**, 1219 (2013).
- [54] J. Toulouse, E. Rebolini, T. Gould, J. F. Dobson, P. Seal, and J. G. Ángyán, *J. Chem. Phys.* **138**, 194106 (2013).
- [55] E. D. Hedegård, F. Heiden, S. Knecht, E. Fromager, and H. J. A. Jensen, *J. Chem. Phys.* **139**, 184308 (2013).
- [56] K. Pernal, *J. Chem. Phys.* **136**, 184105 (2012).
- [57] O. V. Gritsenko, S. J. A. van Gisbergen, A. Görling, and E. J. Baerends, *J. Chem. Phys.* **113**, 8478 (2000).
- [58] N. T. Maitra, F. Zhang, R. J. Cave, and K. Burke, *J. Chem. Phys.* **120**, 5932 (2004).
- [59] M. E. Casida, C. Jamorski, K. C. Casida, and D. R. Salahub, *J. Chem. Phys.* **108**, 4439 (1998).
- [60] A. Dreuw, J. L. Weisman, and M. Head-Gordon, *J. Chem. Phys.* **119**, 2943 (2003).
- [61] E. H. Lieb, *Int. J. Quantum. Chem.* **24**, 24 (1983).
- [62] F. Colonna and A. Savin, *J. Chem. Phys.* **110**, 2828 (1999).
- [63] A. M. Teale, S. Coriani, and T. Helgaker, *J. Chem. Phys.* **130**, 104111 (2009).
- [64] D. P. Joubert and G. P. Strivastava, *J. Chem. Phys.* **109**, 5212 (1998).
- [65] A. Savin, F. Colonna, and M. Allavena, *J. Chem. Phys.* **115**, 6827 (2001).
- [66] A. M. Teale, S. Coriani, and T. Helgaker, *J. Chem. Phys.* **132**, 164115 (2010).
- [67] M. D. Strömsheim, N. Kumar, S. Coriani, E. Sagvolden, A. M. Teale, and T. Helgaker, *J. Chem. Phys.* **135**, 194109 (2011).
- [68] J. Toulouse, F. Colonna, and A. Savin, *Mol. Phys.* **103**, 2725 (2005).
- [69] A. M. Teale, S. Coriani, and T. Helgaker, *J. Chem. Phys.* **133**, 164112 (2010).
- [70] F. Zhang and K. Burke, *Phys. Rev. A* **69**, 052510 (2004).
- [71] P. Gori-Giorgi and A. Savin, *Phys. Rev. A* **73**, 032506 (2006).
- [72] *DALTON, a molecular electronic structure program, Release DALTON2013.0 (2013), see <http://daltonprogram.org>.*

- [73] K. Aidas, C. Angeli, K. L. Bak, V. Bakken, R. Bast, L. Boman, O. Christiansen, R. Cimiraglia, S. Coriani, P. Dahle, et al., *WIREs Comput. Mol. Sci.* (2013), doi: 10.1002/wcms.1172.
- [74] Q. Wu and W. Yang, *J. Theor. Comput. Chem.* **02**, 627 (2003), ISSN 0219-6336.
- [75] K. Kaufmann, *J. Phys. B At. Mol. Opt. Phys.* **24**, 2277 (1991).
- [76] T. H. Dunning, *J. Chem. Phys.* **90**, 1007 (1989).
- [77] See supplementary material for the fits of the total and excitation energies.
- [78] C. Umrigar, A. Savin, and X. Gonze, in *Electronic Density Functional Theory*, edited by J. F. Dobson, G. Vignale, and M. P. Das (Springer US, 1998), pp. 167–176.
- [79] C. Filippi, C. J. Umrigar, and X. Gonze, *J. Chem. Phys.* **107**, 9994 (1997).
- [80] A. Savin, C. J. Umrigar, and X. Gonze, *Chem. Phys. Lett.* **288**, 391 (1998).
- [81] I. Gerber and J. G. Ángyán, *Chem. Phys. Lett.* **415**, 100 (2005).
- [82] A. Görling, *Phys. Rev. A* **54**, 3912 (1996).
- [83] A. Savin, *J. Chem. Phys.* **134**, 214108 (2011).
- [84] A. Savin, *J. Chem. Phys.* **140**, 18A509 (2014).

